

Article

Preparation of a Highly Porous Clay-Based Absorbent for Hazard Spillage Mitigation via Two-Step Expansion of Vermiculite

Duc Cuong Nguyen ¹, Trung Tuyen Bui ², Yeong Beom Cho ¹ and Yong Shin Kim ^{3,*}

¹ Department of Bionano Engineering, Hanyang University, Ansan 15588, Korea; cuongnguyen@hanyang.ac.kr (D.C.N.); youngbumcho@naver.com (Y.B.C.)

² Institute of Natural Science and Technology, Hanyang University, Ansan 15588, Korea; trungtuyen@hanyang.ac.kr

³ Department of Chemical and Molecular Engineering, Hanyang University, Ansan 15588, Korea

* Correspondence: yongshin@hanyang.ac.kr; Tel.: +82-31-400-5507

Abstract: Expanded vermiculite (eVMT) has been studied as a risk-free, general-purpose absorbent for liquid hazards due to its excellent thermal and chemical stability. Here, vermiculite was expanded by two steps: exfoliation by 30 wt% H₂O₂ treatment at 60 °C and subsequent expansion by microwave heating. This two-step expansion produced more homogeneously separated concertina-like eVMTs with a higher total pore volume of 7.75 cm³ g⁻¹ than the conventional thermal method. The two-step eVMT was found to be greatly superior to the thermal and commercial silver counterparts in hazardous liquid-uptake performance. The uptake was simply interpreted as a physical infilling process of a liquid into the eVMT pores, and the spontaneous hazard removal with a great capacity was discussed with the large pore volume of two-step eVMT and its suitable pore dimensions for capillary action. As a practical device, a prototype absorbent assembly made of these eVMTs demonstrated the successful mitigation of liquid hazards on an impermeable surface.

Keywords: expanded vermiculite; absorbent; hazard spillage; H₂O₂ treatment; microwave oven



Citation: Nguyen, D.C.; Bui, T.T.; Cho, Y.B.; Kim, Y.S. Preparation of a Highly Porous Clay-Based Absorbent for Hazard Spillage Mitigation via Two-Step Expansion of Vermiculite. *Minerals* **2021**, *11*, 1371. <https://doi.org/10.3390/min11121371>

Academic Editor: Mercedes Regadío García

Received: 3 November 2021
Accepted: 1 December 2021
Published: 3 December 2021

Publisher's Note: MDPI stays neutral with regard to jurisdictional claims in published maps and institutional affiliations.



Copyright: © 2021 by the authors. Licensee MDPI, Basel, Switzerland. This article is an open access article distributed under the terms and conditions of the Creative Commons Attribution (CC BY) license (<https://creativecommons.org/licenses/by/4.0/>).

1. Introduction

Large-scale chemical spill accidents frequently occur worldwide on land or in oceans during the production, storage, transportation and usage of hazardous chemicals [1]. Sudden hazard spillage not only poses a fatal threat to human life, but also causes serious environmental contamination. Therefore, precautions should be taken in advance for mitigating the risks of spill accidents. Absorbent-based mitigation can efficiently clean up liquid hazards without secondary chemical pollutants that are usually produced in different mitigation methods, such as dispersion, in-situ burning and solidification [2–4]. A great number of absorbents have been developed for the removal of harmful chemical spillages using natural minerals, natural organics, synthetic polymers and carbon nanomaterials [5–15]. Natural organics and synthetic polymers can be degraded by toxic compounds and easily burned by fire, often accompanied by chemical accidents [16]. On the other hand, inflammability and high production cost of carbon nanomaterials hamper their broad utilization as absorbents under harsh conditions [9,10]. Therefore, inorganic minerals, such as zeolites, clays and silicon oxides have been considered as risk-free and general-purpose absorbents for the remediation of liquid hazard spillage due to their ideal properties, including non-flammability, chemical inertness, low environmental impact and a natural abundance. However, they have a crucial drawback. Their absorption capacity is inferior to advanced carbon or polymer absorbents. For realizing a high-performance absorbent, the absorption capacity of the mineral absorbents must be improved.

Vermiculite is a type of natural phyllosilicate clay with a 2:1 layer structure, possessing an octahedral alumina sheet sandwiched by tetrahedral silicate sheets. The trilayer units

with a negative surface charge are bonded together by electrostatic attractions via interlayer metal cations. It can be expandable through the hydration of the interlayer cations and the delamination of the tri-layer units. Its exfoliated form, expanded vermiculite (eVMT), has been proven to be a promising sorbent material for the removal of dyes [17] and metal cations [18] in an aqueous solution, as well as petroleum oils [19,20], and other liquid hazards [7,21]. For attaining high absorptive mitigation capacity, crude vermiculite must be carefully exfoliated to have a great pore volume and appropriate pore sizes. The extent of expansion and pore-size distribution strongly depend on exfoliation methods. There are three major methodologies of thermal heating [22–24], microwave irradiation [25–27], and hydrogen peroxide treatment [28,29]. Flame (or furnace) heated to around 1000 °C and continuous microwave processing are usually utilized in industry for mass production of eVMT. The hydrogen peroxide treatment has been proven to result in the highest expansion ratio among them. This expansion process can be easily modulated by H₂O₂ concentration, reaction time and temperature. Recently, hybrid expansion routes using H₂O₂ and microwave treatments have been reported to exhibit more exfoliated, highly porous eVMTs [30,31]. The pore size existing in eVMT was confirmed to be very important for spontaneous and fast imbibition of a liquid by capillary action [32]. Hence, it remains a challenge to discover an efficient and affordable expansion process, suitable for making highly exfoliated eVMT with optimized pore dimensions.

In this work, a highly exfoliated eVMT was successfully prepared by a two-step expansion process: H₂O₂ treatment followed by microwave drying. Non-expanded Palabora vermiculite was greatly exfoliated in an aqueous solution of 30 wt% H₂O₂ at 60 °C for 1 h, and then expanded further via brief evaporation of the remaining liquid by microwave heating. The two-step expansion resulted in a high expansion magnitude of 20, corresponding to more than three times of the thermal expansion. The two-step eVMTs exhibited a homogeneously exfoliated porous structure with micrometer-sized pore dimensions. Furthermore, their absorption performances were evaluated in terms of their absorption capacity, filling percentage and removal efficiency for twenty hazardous liquid chemicals. These hazards belong to different types of hydrocarbon compounds. They are arbitrarily chosen among sixty-nine accident precaution chemicals that are supervised by the South Korean government, with considerations of their availability and experimental risk. The two-step eVMTs revealed greatly enhanced absorption performances, which is discussed with their observed morphology and pore-size distribution. A prototype absorbent assembly was fabricated and applied to mitigate the liquid compounds existing on an impermeable surface to demonstrate its usefulness as a hazard clean-up device.

2. Materials and Methods

2.1. Chemicals

Crude vermiculite (micro-grade, Palabora mining company, Phalaborwa, South Africa) and silver expanded vermiculite (granules, China) were obtained from Shinsung Mineral (SeongNam, Korea). Ethanol, methyl ethyl ketone, ethyl acetate, furfuryl alcohol, acrylic acid, methyl acrylate, allyl alcohol, acrylonitrile, benzene, toluene, *m*-cresol, isophorone diisocyanate, benzyl chloride, toluene-2,4-diisocyanate, vinyl acetate, and 30 wt% H₂O₂(aq) were purchased from Daejung Chemicals and Metals (Siheung, Korea). Liquified phenol and methyl vinyl ketone were acquired from Sigma-Aldrich. Methanol and allyl chloride were purchased from Junsei Chemical, and 2-nitrotoluene was from Acros Organics. All chemicals were of reagent grade without any further purification.

2.2. Preparation of eVMT Absorbents

Figure 1a shows a schematic diagram for the preparation of eVMT, based on a two-step process consisting of wet H₂O₂ treatment and microwave drying. Very thin or tiny vermiculite particles were discarded by means of a weight-based separation for better homogeneity in the sample dimension. The refined non-expanded vermiculite was first treated with an aqueous solution of 30 wt% H₂O₂ for its chemical exfoliation. Typically,

10 g of the sample was spread in a glass Petri dish (diameter = 150 mm) containing a 60 mL H_2O_2 solution, and then placed in a convection oven at 60 °C for 1 h covered by a lid. Next, the dish was transferred to a 1 kW microwave oven (KR-S341T, Daewoo, South Korea) in order to quickly evaporate the liquid solution. The wet-treated sample was heated by microwave radiation for 60 s. Afterward, the heated sample (~100 °C) was taken out in ambient atmosphere for cooling and further evaporation. This heating-cooling cycle was sequentially performed around five times until liquid was almost completely evaporated. The H_2O_2 -expanded sample was finally dried at 150 °C in a vacuum oven for 1 h, and then stored in a desiccator before usage. For a comparison study, thermally expanded vermiculite at 1000 °C and a commercial silver sample were also utilized. The detailed thermal expansion conditions were previously reported for the same crude vermiculite [7].

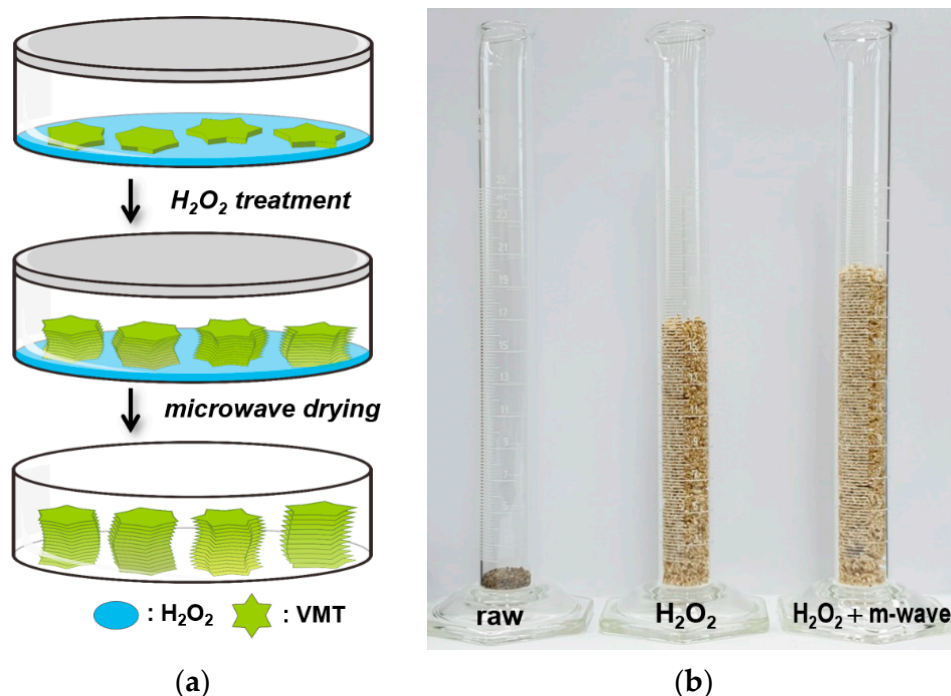


Figure 1. (a) Schematic diagram of the two-step process used for the preparation of highly expanded vermiculite. (b) Photographs displaying 1 g of vermiculite: non-expanded raw sample (left), expanded samples taken after the first H_2O_2 treatment (middle) and the second microwave drying (right).

2.3. Material Characterizations

The extent of the expansion of vermiculite was evaluated by measuring the change in volume [33], as shown in Figure 1b. To obtain an initial sample volume (V_0), 1 g of the crude vermiculite was put into a graduated cylinder. The expanded volume after the H_2O_2 and microwave treatments (V) was also quantified by a graduated cylinder. The volumes were measured after tipping samples gently for packing, and their average values were obtained from five measurements. The expansion ratio (k) was calculated by the relationship of $k = V/V_0$.

The morphology of eVMT was observed by scanning electron microscopy (SEM; S-4800, Hitachi, Tokyo, Japan) under an electron beam with an accelerating voltage of 15 kV after deposition of a platinum nano-film. The chemical compositions of vermiculite were analyzed by X-ray fluorescence (XRF; ZSX Primus II, Rigaku, Tokyo, Japan). Crystal structures of the samples were probed by powder X-ray diffractometer (PXRD; Uniflex 600, Rigaku) with $Cu-K\alpha_1$ ($\lambda = 1.54056 \text{ \AA}$) radiation. Nitrogen sorption (Belsorp-mini II, Micromeritics, Tokyo, Japan) and mercury porosimetry (AutoPore IV 9500, Micromeritics,

Norcross, GA, USA) were utilized to characterize pore size distribution and a specific surface area.

2.4. Absorptive Removal Performance against Liquid Hazards

The absorption capacities and removal efficiencies of the three eVMTs were evaluated for 20 types of harmful liquid chemicals. The detailed experimental procedures were reported in [7]. Briefly, a stainless-steel mesh cell was charged by a 1.0 g eVMT sample, then fully immersed into a testing liquid for 30 min. It was lifted up to allow the excess liquid drained off. Shortly afterward, the weight of absorbed samples (M_{abs}) was measured by a balance. The dry mass (M_{dry}) was determined after drying in a vacuum oven at 150 °C for 1 h. The absorption capacity, defined by the relative weight of the absorbed liquid to absorbent, was determined by the following relationship.

$$\text{Absorption capacity (g g}^{-1}\text{)} = \frac{M_{abs} - M_{dry}}{M_{dry}} \quad (1)$$

These weights were determined by averaging values acquired by three measurements.

For determining the removal efficiency, approximately 20 g of hazardous liquid was prepared in a reservoir. Its initial weight (M_i) was measured by a balance. A meshed container was filled with 10 g eVMT and then immersed into the hazard-containing vessel for 10 min. The eVMT container was lifted up and waits for dripping the excess liquid. The weight of the remaining solvent (M_r) was measured. The removal efficiency was defined by the percentage ratio of the extracted liquid mass with respect to its initial quantity, which was calculated by the following equation.

$$\text{Removal efficiency (\%)} = \frac{M_i - M_r}{M_i} \times 100 \quad (2)$$

2.5. Fabrication and Demonstration of a Prototype Absorbent Assembly

A prototype absorbent assembly was fabricated to reveal the real application of eVMT as an absorbent for liquid hazard mitigation. Figure 2a shows the unlocked assembly consisting of an absorbent paper pouch and a stainless-steel mesh container. The absorbent pouch with a dimension of width \times depth \times height = 50 \times 35 \times 65 mm³ was filled up by 7 g eVMT and was then sealed using a hand-press sealing machine. The pouch was placed inside of a stainless-steel mesh container (ϕ = 65 mm and h = 65 mm) and confined by a locked structure. The strong, heavy stainless-steel holder provides advantages to increase the specific gravity of the assembly for quick submersion and to handle it reliably. A hazard mitigation test of the prototype device was performed under the following protocol: (1) immersing the assembly into a beaker containing 300 mL of a liquid organic chemical for 1 min, (2) withdrawing it outside the beaker and measuring a weight of remaining liquid and (3) repeating the mitigation cycle (steps 1 and 2) using a new assembly until the beaker became nearly empty. The mitigation procedure can see in Video S1 in the Supplementary Materials. Figure 2b shows the experimental setup used for the mitigation test after the first mitigation of a blue-dyed ethanol solution. The absorption capacity of each mitigation trial and the cumulative removal efficiency were calculated from the measured weights.



Figure 2. (a) Picture of the unlocked prototype absorbent assembly consisting of a stainless-steel mesh container and an absorbent paper pouch made of eVMTs. (b) Image of the experimental setup for a liquid mitigation test using the prototype absorbent assembly. The solution was intentionally colored by a blue dye for visibility.

3. Results and Discussion

3.1. Expansion Behavior of Palabora Vermiculite

The expansion ratio was measured at different temperatures and times of H_2O_2 exfoliation under a subsequent thermal drying. Figure 3 shows variations of the expansion ratio as a function of the H_2O_2 reaction time obtained at three different temperatures of 25 °C, 60 °C and 80 °C. At the lowest temperature of 25 °C, the k magnitude steadily increased and reached 8.0 at a reaction time of 3 h. As the temperature increased, the expansion happened more quickly and was then saturated to a maximum value: $k = 16.2$ at a reaction time of 1 h and $k = 15.4$ at 0.5 h for expansion at 60 °C and 80 °C, respectively. A more rapid expansion at a higher temperature was previously reported and interpreted as the efficient evolution of atomic oxygen via decomposition of hydrogen peroxide penetrated into the interlayer spaces of vermiculite [29]. The atomic oxygen could result in the separation of the silicate layers from each other. On the other hand, the maximum k magnitude at 80 °C was slightly lower than that at 60 °C. This behavior seems to be attributed to a decrease in H_2O_2 concentration with the elapse of reaction time due to the considerable H_2O_2 decomposition outside of the interlayer. The expansion was known to greatly diminish below the concentration of 30 wt% H_2O_2 [28]. In addition, extremely exfoliated vermiculites were observed to break down to smaller fragments at 80 °C, which resulted in a decrease in k magnitude. As a result, the 60 °C H_2O_2 treatment for 1 h was chosen as an optimized exfoliation condition, and utilized to prepare highly expanded, mechanically durable vermiculite.

A volume shrinkage of the H_2O_2 treated sample was observed during the subsequent thermal drying, induced by the evaporation of water molecules with a high surface tension. For preventing the shrinkage and reducing the dry process time, H_2O_2 -treated particles were dried by the heating-cooling cycle of the microwave irradiation for 1 min and standing in ambient air for 1 min. Complete drying was possible within approximately 10 min. Interestingly, the sample was found to be further expanded during the microwave drying process: the volume was increased by approximately 23% when compared with that after the H_2O_2 treatment (see Figure 1b). The k values of three different eVMTs used in this work are summarized in Table 1, together with their physical dimensions and apparent density. The two-step method results in a highly expanded sample up to $k = 20$ while preserving its porous structure. Compared with the $k = 6.6$ obtained from thermally expanded samples at 1000 °C, the two-step expansion provides a higher k magnitude of more than three times for the same Palabora vermiculite. The microwave expansion has been previously reported in several different types of vermiculites [24–26]. This process can be understood as a result of the build-up pressure formed by the prompt evaporation of crystal water remaining in the vermiculite interlayers after H_2O_2 treatment. Therefore, H_2O_2 treatment coupled with

microwave drying is an efficient method to prepare a highly porous, robust absorbent for the mitigation of liquid hazards.

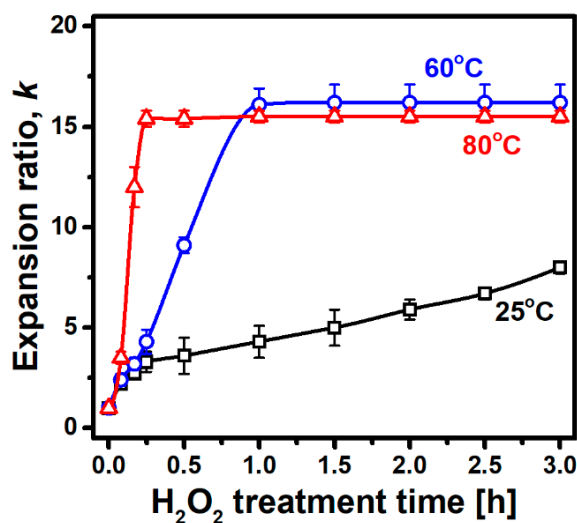


Figure 3. Variations of expansion ratios as a function of a H₂O₂ treatment time at three different temperatures.

Table 1. Summary on dimensions, apparent density and expansion ratio of the used eVMTs.

Sample Preparation	Planar Size ^a [mm]	Thickness ^b [mm]	Apparent Density [g cm ⁻³]	Expansion Ratio, <i>k</i>
Two-step method	0.48	0.11	0.050	20
Thermal heating	0.84	0.15	0.151	6.6
Commercial Silver	1.32	-	0.167	6.0 ^b

^a An average value was obtained from 50 samples using a digital caliper or a micrometer. ^b Estimated using the bulk density of crude Palabora vermiculite.

3.2. Characterization of Material Properties

SEM images of the eVMTs prepared by the two-step process and the rapid 1000 °C heating are shown in Figure 4a,b, respectively. The image obtained from the two-step expansion reveals a morphology with a more homogeneously separated concertina-like shape than that of the thermal expansion. The conical slit gaps have an opening size of less than 250 μm and the thickness of the unexfoliated flakes is in the range of 0.1–0.4 μm. The plate thickness is thinner than that of the thermally expanded sample, indicating more favorable interlayer delamination of the crude vermiculite. This observation is in good agreement with the greater expansion ratio of the two-step sample. These results indicate that H₂O₂ treatment coupled with microwave drying can produce more uniform and extensive exfoliation of vermiculite interlayers than simple thermal expansion. In addition, the chemical compositions analyzed by XRF are given in Table 2. The obtained compositions are in good agreement with previously reported results for the same vermiculite [22,28,34].

Porous characteristics of eVMTs were quantitatively evaluated by both Hg porosimetry and N₂ sorption. Figure 5a shows pore-size distributions of the two-step and the thermally expanded samples quantified by Hg porosimetry. They display bimodal distributions: two peaks at 7.0 μm and 260 μm for the two-step sample, and two maxima at 1.9 μm and 284 μm for the thermal sample. These distributions exhibit a macropore component in the region larger than approximately 100 μm together with the small pores. The macroporosity might be considered as interparticle voids formed by packing eVMT granules. More importantly, the two-step sample presents higher intensity in intrusion volume, suggesting the existence of a larger pore volume within eVMT, than that of the thermal one. A total pore volume of 7.75 cm³ g⁻¹ was obtained from the two-step sample, more than two times greater when compared to the thermal sample. These total pore volumes and areas are

summarized in Table 3, together with complementary values analyzed by N₂ sorption. These distributions clearly indicate that the two-step eVMT has a highly porous structure with a pore dimension of 0.1–500 μm, as observed by SEM.

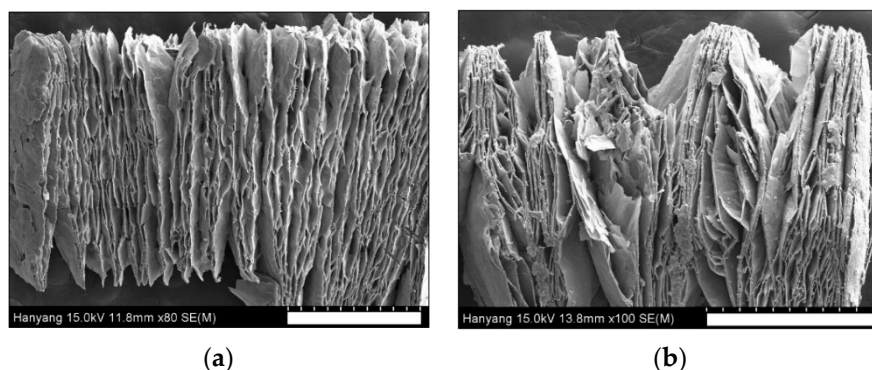


Figure 4. SEM images of Palabora vermiculite expanded by (a) H₂O₂ treatment followed by microwave drying, and (b) thermal treatment at 1000 °C. The white scale bars correspond to 500 μm.

Table 2. Chemical compositions of raw Palabora vermiculite analyzed by XRF.

	SiO ₂	MgO	Al ₂ O ₃	K ₂ O	FeO	TiO ₂	CaO	Na ₂ O	MnO	NiO	Cr ₂ O ₃
Content [wt%]	42.1	17.4	11.0	8.6	15.6	2.2	2.4	0.33	0.13	0.06	0.08

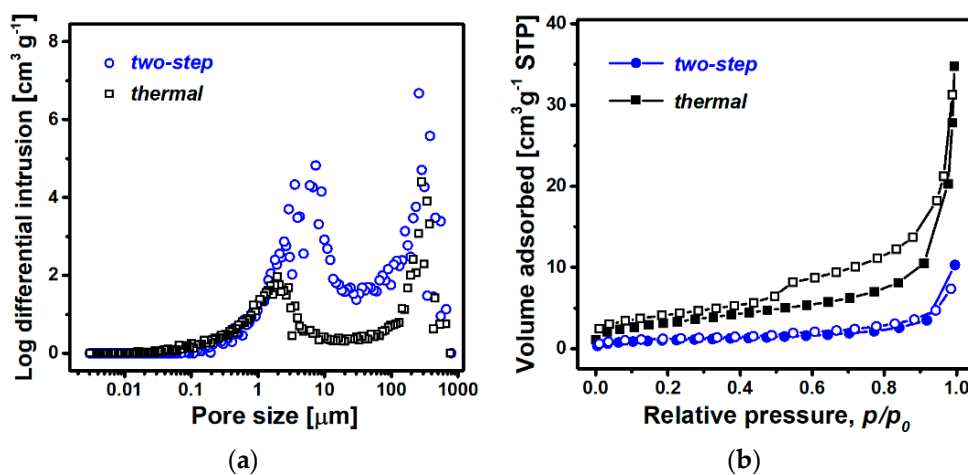


Figure 5. Pore-size distributions of the two-step and thermal eVMTs analyzed by (a) Hg porosimetry and (b) N₂ sorption.

Table 3. Summary of the porosity characteristics of the two eVMTs probed by Hg porosimetry and N₂ sorption.

Analysis Method	Properties	Two-Step	Heating
Hg porosimetry	Total pore volume [cm ³ g ⁻¹]	7.75	3.65
	Total pore area [m ² g ⁻¹]	8.38	13.0
N ₂ sorption	Total pore volume [cm ³ g ⁻¹]	0.015	0.046
	BET surface area [m ² g ⁻¹]	3.57	11.8

Furthermore, for investigating the distribution of pores smaller than sub-micrometer, N₂ sorption isotherms of the two samples were measured as shown in Figure 5b. In contrast to Hg porosimetry, the isotherm curve of the thermal sample exhibits higher intensity in

adsorption volume and a more obvious hysteresis loop in the region of $p/p_0 = 0.4$ – 0.95 than those of the two-step sample. The higher adsorption indicates that the smaller pore structure is more extensively developed during the thermal expansion than the counterpart. This interpretation is well supported by the values of the surface area and total pore volume, obtained from the BET adsorption model (see Table 3). The thermal sample has a BET surface area of $11.8 \text{ m}^2 \text{ g}^{-1}$, which is greater than the $3.57 \text{ m}^2 \text{ g}^{-1}$ of the two-step. On the other hand, the hysteresis loop suggests the existence of a mesoporous structure, and the BJH analysis exhibited a distinct peak at around 30 nm in pore-size distribution (see Figure S1). These results indicate that the porosity characteristics are strongly dependent on the expansion method used: the H_2O_2 -treatment coupled with the microwave drying method produces a highly expanded form with various conical slit gaps in micrometer dimensions, whereas the thermal expansion is favorable to provide a micro/mesoporous structure with a large surface area. The two-step eVMT with a large total pore volume seems to be a promising absorbent for liquid hazard removal. In addition, the thermally expanded sample may have many advantages in surface-involved adsorption applications.

Figure 6 shows the PXRD spectra of the crude and two eVMTs in a low 2θ angle region for observing a change in the first-order basal spacing (d_{002}). The crude sample exhibits three intense reflections with d -spacings of 1.43 nm, 1.25 nm and 1.19 nm and one weak peak of $d_{002} = 1.01$ nm. These different d -spacings have been interpreted with different water-layer hydration-states (WLHS) and interstratification: 2-WLHS for 1.43 nm, interstratified phase for 1.25 nm, 1-WLHS for 1.19 nm and 1/0-WLHS for 1.01 nm [22,25,35]. In the case of the two-step eVMT, the four peaks still survive with a slight broadening, indicating the occurrence of significant exfoliation of the basal layers without a serious change in crystalline structure. In addition, the decrease in the 2-WLHS peak intensity implies that the H_2O_2 and subsequent microwave treatments induce a slight diminishment in the hydrated states of the interplanar cations. Similar intensity reduction was previously reported more clearly when a Mg-vermiculite sample was treated by 80°C $\text{H}_2\text{O}_2(\text{aq})$ and microwave radiation for 40 min [31]. The high H_2O_2 temperature and the long microwave time may be attributed to induce great exfoliation and extensive water evaporation from the fully hydrated 2-WLHS, respectively. In contrast, the PXRD pattern of the thermal sample displays only the dehydrated 1/0-WLHS peak with the smallest d -spacing. The hydrated and interstratified peaks completely disappeared. These observations are in good agreement with the previous works [7,22]. The prompt heating seems to cause almost complete dehydration and break-down of the interstratified structure. Consequently, the resultant crystal structures of the eVMTs could be related with the above-mentioned different characteristics in porosity according to the expansion methods.

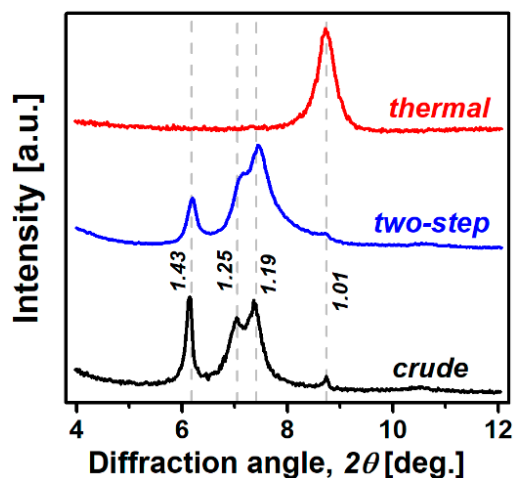


Figure 6. PXRD patterns of crude vermiculite and its two expanded forms prepared by H_2O_2 treatment coupled with microwave drying and prompt heating. The designated values correspond to d -spacings at the nanometer scale.

3.3. Hazardous Liquid-Uptake Performances

3.3.1. Absorption Capacity

The absorption capacity of the two-step eVMT was quantified for twenty harmful organic compounds with different chemical properties, including ethanol, methanol, methyl ethyl ketone, ethyl acetate, furfuryl alcohol, acrylic acid, methyl acrylate, phenol, allyl alcohol, methyl vinyl ketone, acrylonitrile, benzene, toluene, *m*-cresol, allyl chloride, 2-nitrotoluene, isophorone diisocyanate, benzyl chloride, toluene-2,4-diisocyanate and vinyl acetate. The same measurements were also performed using thermally expanded and commercial silver eVMTs for the purpose of comparison. Figure 7 shows horizontal bar graphs for the liquid hazards, displaying variations in the absorption capacity for the three eVMTs. The hazardous compounds are arbitrarily grouped together according to the hydrophilicity. Hydrophilic and hydrophobic chemicals are positioned in the upper and bottom regions of the graph, respectively. The two-step sample distinctly exhibits great absorption capacities, ranging from 2.4 g g⁻¹ to 7.9 g g⁻¹. These capacities are approximately 2–3 times higher than those of the thermal and silver samples for the same chemical, except for the three hydrophobic chemicals of isophorone diisocyanate, benzyl chloride and toluene-2,4-diisocyanate with a lower capacity of less than 4.0 g g⁻¹. There is no clear correlation with the absorption capacity and chemical properties of an absorbate, such as hydrophilicity/hydrophobicity and the existence of a specific functional group, as in our previous results obtained from the thermally expanded sample [7]. Although it is not a major factor, the inferior absorption capability to the specific hydrophobic compounds suggests that the absorption can be affected by chemical interactions between the liquid hazard and eVMT. In addition, the obtained absorption capacities for various hazards are greater than 0.53 g g⁻¹ of hydrophobic dolomite [12] for oil and 2.5 g g⁻¹ of modified VMT [20] for water, and comparable with 3.2–7.5 g g⁻¹ of expanded perlite [6] for oil–water mixture.

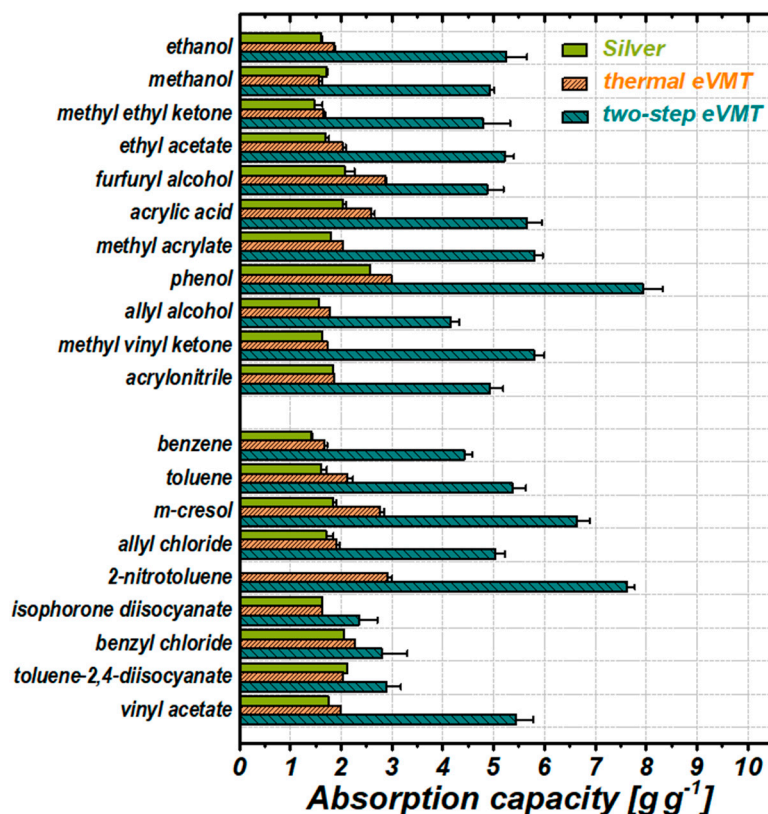


Figure 7. Horizontal bar charts displaying the absorption capacities of three different eVMTs for various hazardous liquid chemicals. The error bars were obtained using three measurements.

Assuming that the absorption happens by infilling the macro-porous total pore volume of eVMT, the absorption capacity defined by the relative weights strongly depends on the density of a liquid hazard. The total pore volume (V_t) of $7.75 \text{ cm}^3 \text{ g}^{-1}$ determined by Hg porosimetry corresponds to the maximum amount in absorption volume capacity, i.e., absorbed volume per unit of absorbent weight. The filling percentage of the pore volume can be expressed by the following equation:

$$\text{Filling percentage (\%)} = \frac{V}{V_t} \times 100 \quad (3)$$

where V is the absorbed liquid volume per 1 g eVMT. This value can be calculated by the division of the absorption capacity (g g^{-1}) by the liquid density (g cm^{-3}). Figure 8 displays the variations of the filling percentages for the two-step and the thermally expanded samples. Overall, the two-step eVMT exhibits higher filling percentages than those of the thermal one, presenting better efficiency in absorptive liquid uptake. However, the filling percentage exhibits an opposite tendency in the case of furfuryl alcohol and the three hydrophobic compounds with a low absorption capacity, which is further evidence for the involvement of the chemical characteristics of a hazard in an absorption process. The two-step eVMT demonstrates a high filling percentage of 63–96%, except for the four exceptions.

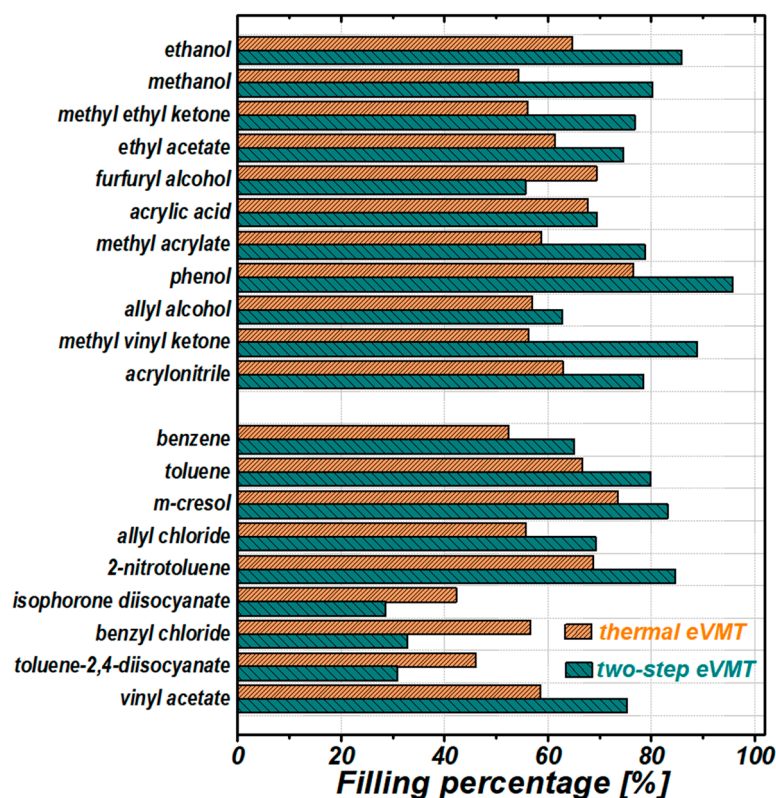


Figure 8. Horizontal bar charts displaying the filling percentage of a total pore volume of two-step and thermal eVMTs for various hazardous liquid chemicals.

3.3.2. Removal Efficiency

The removal efficiencies of the three eVMTs were also measured for the same harmful chemicals in order to evaluate the effectiveness in hazard removal via spontaneous wicking. The obtained quantities are presented in Figure 9. The removal efficiency of the two-step sample is greater than 95% for all the tested chemicals, which discloses a superb capability in hazard removal. In addition, the removal efficiency reveals a little variation in magnitude,

irrespective of the tested hazardous chemicals. This outcome outperforms 90% of the thermal eVMT and 73–95% of silver.

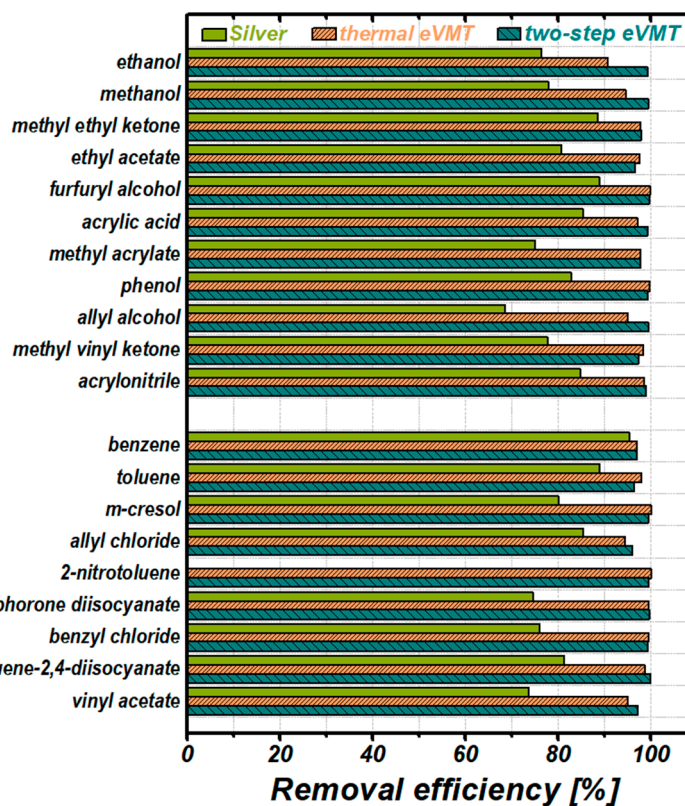


Figure 9. Horizontal bar charts displaying the removal efficiencies of three different eVMTs for various hazardous liquid chemicals.

3.3.3. Analysis of the Absorption Performance

The absorption capacity has a strong correlation with the total pore volume of eVMT and the density of hazardous liquids rather than any other physicochemical properties. Therefore, the adsorption can be regarded as the physical process of infilling a liquid hazard into the pores of eVMT, even though it is slightly affected by chemical interactions between the absorbent and absorbate. For preparing eVMT with a great absorption capacity, one of the most important requirements is a high expansion ratio, i.e., the great pore volume in eVMT. Another key factor is the size distribution of the pores. Since liquid wicking behavior strongly depends on the dimensions of a flow channel, the size of the empty gaps in eVMT can influence the absorption characteristics, such as the filling percentage and the removal rate. In fact, the spontaneous imbibition degrades along a channel that is too narrow or wide due to the considerable flow resistance or negligible capillarity, respectively. An ideal eVMT pore size for absorptive hazard removal seems to be in the micrometer range of roughly 1–100 μm .

In studying the hazard uptake performance, the two-step sample demonstrates the best performance among the three eVMTs in terms of the absorption capacity, the filling percentage and the removal efficiency. The excellent performances can be interpreted as an outcome of producing a highly and uniformly expanded structure with a large pore volume of $7.75 \text{ cm}^3 \text{ g}^{-1}$ with suitable conical slit gaps of 0.1–500 μm for capillary action. It is worth remembering that thermal eVMT with a larger surface area does not result in higher absorption capacity. The weak dependence of uptake behaviors on hydrophilicity or hydrophobicity can be explained with the unique wetting property of eVMT having both superhydrophilicity and oleophilicity, as observed in our previous work [32]. Hydrophobic organic molecules have been observed to spontaneously penetrate into a physically packed

eVMT column, although the flow rate is slower than that of aqueous solution. Consequently, these uptake tests obviously indicate that the two-step eVMT can be utilized as an effective absorbent for the remediation of various types of liquid hazards.

3.4. Hazard Mitigation Using the Prototype Absorbent

The prototype absorbent assembly was fabricated to determine its usefulness as a remedy for a liquid hazard existing on an impermeable surface. Video S1 demonstrates the almost complete removal of a 300 mL ethanol solution in a beaker via eight consecutive mitigations using a new eVMT assembly each time. Because the submersion and take-out times were controlled to be 1 min, the total process time was approximately 16 min. A metal chain linked to the mesh container was utilized to effectively move the assembly. Using an absorbent weight of about 7 g and the measured weight of the remaining liquid, the absorption capacity and the cumulative removal efficiency of each mitigation trial were calculated and are given in Table 4. This mitigation test was also performed for different chemicals of methanol, acrylonitrile, toluene and vinyl acetate. In spite of the short absorption time of 1 min, absorption capacities of the first mitigation were in the range of 5.9–7.2 g g⁻¹, slightly higher than the corresponding values for the same chemicals (see Figure 7). This range can be ascribed to the use of different amounts of absorbent and absorbate, and/or a dissimilar type in the absorbent container. The sorption capacity obviously decreased and the cumulative removal efficiency increased as the mitigation was repeated several times. The decrease in absorption capacity was due to the reduction in the liquid volume. It is worth mentioning that the assembly can absorb a considerable amount of chemicals for 1 min via spontaneous wicking action even when it is partially in contact with a small amount of liquid. All the tested chemicals exhibit cumulative removal efficiencies greater than 97% after six or seven consecutive mitigations. These tests successfully reveal that the eVMT-based prototype device can be utilized to remedy the spillage of various harmful organic compounds on an impermeable floor or soil. Because the absorbent assembly made of granular eVMT particles is reusable after thermal activation and can be flexibly fabricated with diverse sizes and shapes, our prototype device has the potential to become a cost-effective solution to safely remove various liquid hazards.

Table 4. Summary on mitigation performance of the prototype absorption assembly for five different organic compounds.

Chemicals	Uptake Performance	No. of Mitigation Trial						
		1	2	3	4	5	6	7
Ethanol	absorption capacity [g g ⁻¹]	6.35	5.69	5.12	4.50	4.50	3.43	2.82
	removal efficiency ^a [%]	18.3	33.3	50.0	63.3	78.3	88.3	97.0
Methanol	absorption capacity [g g ⁻¹]	5.94	5.37	5.40	4.98	4.88	3.55	1.92
	removal efficiency ^a [%]	16.7	33.3	50.0	66.7	83.3	91.7	98.3
Acrylonitrile	absorption capacity [g g ⁻¹]	6.55	6.12	6.05	5.82	5.12	4.21	0.43
	removal efficiency ^a [%]	16.7	33.3	50.0	66.7	83.3	98.3	99.6
Toluene	absorption capacity [g g ⁻¹]	7.19	6.87	6.61	6.59	4.86	4.07	
	removal efficiency ^a [%]	20.0	36.7	63.3	75.0	90.0	98.3	
Vinyl acetate	absorption capacity [g g ⁻¹]	6.01	7.04	6.45	6.00	4.60	4.61	3.29
	removal efficiency ^a [%]	16.7	33.3	50	66.7	78.3	91.7	99.7

^a Calculated with an initial volume of 300 mL and corresponding to the cumulative removal efficiency.

4. Conclusions

The eVMT absorbent was prepared by the two-step method of H₂O₂ treatment coupled with microwave drying as a remedy for hazard spillage. When compared with the conventional thermal expansion, the novel two-step process produced highly and uniformly exfoliated eVMTs with a greater pore volume and more suitable micro-sized pores for capillarity-driven imbibition. These porosity characteristics lead to excellent uptake performance (the absorption capacity = 4.0–7.9 g g⁻¹, the filling percentage = 63–96% and

the removal efficiency >95%) for almost all types of tested harmful liquids. The prototype eVMTs assembly has presented fast, spontaneous removal of liquid organic compounds in a beaker. These results indicate that the eVMTs prepared by the two-step method is a promising general-purpose, risk-free absorbent for a large-scale remediation of hazard spillage due to its low cost, thermal stability, chemical inertness and mechanical durability. In addition, this two-step process could easily scale up using a larger reactor and a bigger microwave processor.

Supplementary Materials: The following are available online at <https://www.mdpi.com/article/10.3390/min11121371/s1>, Figure S1: pore size distributions of the two-step and thermal eVMTs obtained by BJH model, Video S1: the consecutive uptake mitigation of an ethanol solution in a beaker using 8 prototype absorbent assemblies.

Author Contributions: Conceptualization, D.C.N., Y.B.C. and Y.S.K.; methodology, D.C.N. and T.T.B.; validation, D.C.N., T.T.B., Y.B.C. and Y.S.K.; formal analysis, D.C.N. and T.T.B.; investigation, D.C.N. and Y.B.C.; writing—original draft preparation, D.C.N.; writing—review and editing, Y.S.K.; supervision, Y.S.K.; project administration, Y.S.K.; funding acquisition, Y.S.K. All authors have read and agreed to the published version of the manuscript.

Funding: This work was supported by the GRRC program of Gyeonggi Province. [GRRC-HY2021-B04, Development of hydrogen sensing technology for safety].

Data Availability Statement: The data presented in this study are available on request.

Conflicts of Interest: The authors declare no conflict of interest.

References

- Li, Y.; Ping, H.; Ma, Z.-H.; Pan, L.-G. Statistical analysis of sudden chemical leakage accidents reported in China between 2006 and 2011. *Environ. Sci. Pollut. Res.* **2014**, *21*, 5547–5553. [CrossRef]
- Oliveira, L.M.; Saleem, J.; Bazargan, A.; Duarte, J.L.d.S.; McKay, G.; Meili, L. Sorption as a rapidly response for oil spill accidents: A material and mechanistic approach. *J. Hazard. Mater.* **2020**, *407*, 124842. [CrossRef]
- Bandura, L.; Wozzuk, A.; Kołodziejka, D.; Franus, W. Application of mineral sorbents for removal of petroleum substances: A review. *Minerals* **2017**, *7*, 37. [CrossRef]
- Hoang, A.T.; Nguyen, X.P.; Duong, X.Q.; Huynh, T.T. Sorbent-based devices for the removal of spilled oil from water: A review. *Environ. Sci. Pollut. Res.* **2021**, *28*, 28876–28910. [CrossRef]
- Melvold, R.; Gibson, S. A guidance manual for selection and use of sorbents for liquid hazardous substance releases. *J. Hazard. Mater.* **1988**, *17*, 329–335. [CrossRef]
- Bastani, D.; Safekordi, A.; Alihosseini, A.; Taghikhani, V. Study of oil sorption by expanded perlite at 298.15 K. *Sep. Purif. Technol.* **2006**, *52*, 295–300. [CrossRef]
- Cuong, N.D.; Hue, V.T.; Kim, Y.S. Thermally expanded vermiculite as a risk-free and general-purpose sorbent for hazardous chemical spillages. *Clay Miner.* **2019**, *54*, 235–243. [CrossRef]
- Radetic, M.; Ilic, V.; Radojevic, D.; Miladinovic, R.; Jovic, D.; Jovancic, P. Efficiency of recycled wool-based nonwoven material for the removal of oils from water. *Chemosphere* **2008**, *70*, 525–530. [CrossRef] [PubMed]
- Bi, H.; Xie, X.; Yin, K.; Zhou, Y.; Wan, S.; He, L.; Xu, F.; Banhart, F.; Sun, L.; Ruoff, R.S. Spongy graphene as a highly efficient and recyclable sorbent for oils and organic solvents. *Adv. Funct. Mater.* **2012**, *22*, 4421–4425. [CrossRef]
- Ren, R.-P.; Li, W.; Lv, Y.-K. A robust, superhydrophobic graphene aerogel as a recyclable sorbent for oils and organic solvents at various temperatures. *J. Colloid Interface Sci.* **2017**, *500*, 63–68. [CrossRef]
- Wu, Z.-Y.; Li, C.; Liang, H.-W.; Zhang, Y.-N.; Wang, X.; Chen, J.-F.; Yu, S.-H. Carbon nanofiber aerogels for emergent cleanup of oil spillage and chemical leakage under harsh conditions. *Sci. Rep.* **2014**, *4*, 4079. [CrossRef]
- Davoodi, S.M.; Taheran, M.; Brar, S.K.; Galvez-Cloutier, R.; Martel, R. Hydrophobic dolomite sorbent for oil spill clean-ups: Kinetic modeling and isotherm study. *Fuel* **2019**, *251*, 57–72. [CrossRef]
- Shi, Y.; Sun, M.; Liu, C.; Fu, L.; Lv, Y.; Feng, Y.; Huang, P.; Yang, F.; Song, P.; Liu, M. Lightweight, amphiphatic and fire-resistant prGO/MXene spherical beads for rapid elimination of hazardous chemicals. *J. Hazard. Mater.* **2022**, *423*, 127069. [CrossRef]
- Jahanban-Esfahlan, A.; Jahanban-Esfahlan, R.; Tabibiazar, M.; Roufegarinejad, L.; Amarowicz, R. Recent advances in the use of walnut (*Juglans regia* L.) shell as a valuable plant-based bio-sorbent for the removal of hazardous materials. *RSC Adv.* **2020**, *10*, 7026–7047. [CrossRef]
- Ion, I.; Bogdan, D.; Mincu, M.M.; Ion, A.C. Modified exfoliated carbon nanoplatelets as sorbents for ammonium from natural mineral waters. *Molecules* **2021**, *26*, 3541. [CrossRef] [PubMed]
- Herrick, E.C.; Carstea, D.; Goldgraben, G. *Sorbent Materials for Cleanup of Hazardous Spills*; Environmental Protection Agency: Cincinnati, OH, USA, 1982; pp. 25–44.

17. Duman, O.; Tunç, S.; Polat, T.G. Determination of adsorptive properties of expanded vermiculite for the removal of CI Basic Red 9 from aqueous solution: Kinetic, isotherm and thermodynamic studies. *Appl. Clay Sci.* **2015**, *109*, 22–32. [[CrossRef](#)]
18. Marcos, C.; Rodríguez, I. Thermoexfoliated commercial vermiculites for Ni²⁺ removal. *Appl. Clay Sci.* **2016**, *132–133*, 685–693. [[CrossRef](#)]
19. Da Silva, U.G.; Melo, M.A.D.F.; da Silva, A.F.; de Farias, R.F. Adsorption of crude oil on anhydrous and hydrophobized vermiculite. *J. Colloid Interface Sci.* **2003**, *260*, 302–304. [[CrossRef](#)]
20. Purceno, A.D.; Barrioni, B.R.; Dias, A.; da Costa, G.M.; Lago, R.M.; Moura, F.C. Carbon nanostructures-modified expanded vermiculites produced by chemical vapor deposition from ethanol. *Appl. Clay Sci.* **2011**, *54*, 15–19. [[CrossRef](#)]
21. Machado, L.C.R.; Lima, F.W.J.; Paniago, R.; Ardisson, J.D.; Sapag, K.; Lago, R.M. Polymer coated vermiculite–iron composites: Novel floatable magnetic adsorbents for water spilled contaminants. *Appl. Clay Sci.* **2006**, *31*, 207–215. [[CrossRef](#)]
22. Marcos, C.; Arango, Y.C.; Rodriguez, I. X-ray diffraction studies of the thermal behaviour of commercial vermiculites. *Appl. Clay Sci.* **2009**, *42*, 368–378. [[CrossRef](#)]
23. El Mouzdahir, Y.; Elmchaouri, A.; Mahboub, R.; Gil, A.; Korili, S. Synthesis of nano-layered vermiculite of low density by thermal treatment. *Powder Technol.* **2009**, *189*, 2–5. [[CrossRef](#)]
24. Marcos, C.; Rodríguez, I. Expansion behaviour of commercial vermiculites at 1000 °C. *Appl. Clay Sci.* **2010**, *48*, 492–498. [[CrossRef](#)]
25. Udoudo, O.; Folorunso, O.; Dodds, C.; Kingman, S.; Ure, A. Understanding the performance of a pilot vermiculite exfoliation system through process mineralogy. *Miner. Eng.* **2015**, *82*, 84–91. [[CrossRef](#)]
26. Obut, A.; Girgin, I.; Yörükoğlu, A. Microwave exfoliation of vermiculite and phlogopite. *Clays Clay Miner.* **2003**, *51*, 452–456. [[CrossRef](#)]
27. Folorunso, O.; Dodds, C.; Dimitrakis, G.; Kingman, S. Continuous energy efficient exfoliation of vermiculite through microwave heating. *Int. J. Miner. Process.* **2012**, *114–117*, 69–79. [[CrossRef](#)]
28. Obut, A.; Girgin, İ. Hydrogen peroxide exfoliation of vermiculite and phlogopite. *Miner. Eng.* **2002**, *15*, 683–687. [[CrossRef](#)]
29. Üçgül, E.; Girgin, İ. Chemical exfoliation characteristics of Karakoc phlogopite in hydrogen peroxide solution. *Turk. J. Chem.* **2002**, *26*, 431–440.
30. Marcos, C.; Rodríguez, I. Exfoliation of vermiculites with chemical treatment using hydrogen peroxide and thermal treatment using microwaves. *Appl. Clay Sci.* **2014**, *87*, 219–227. [[CrossRef](#)]
31. Weiss, Z.; Valaskova, M.; Seidlerova, J.; Supova-Kristkova, M.; Sustai, O.; Matejka, V.; Capkova, P. Preparation of vermiculite nanoparticles using thermal hydrogen peroxide treatment. *J. Nanosci. Nanotechnol.* **2006**, *6*, 726–730. [[CrossRef](#)] [[PubMed](#)]
32. Nguyen, D.C.; Bui, T.T.; Cho, Y.B.; Kim, Y.S. Highly hydrophobic polydimethylsiloxane-coated expanded vermiculite sorbents for selective oil removal from water. *Nanomaterials* **2021**, *11*, 367. [[CrossRef](#)]
33. Justo, A.; Maqueda, C.; Pérez Rodríguez, J.L.; Morillo, E. Expansibility of some vermiculites. *Appl. Clay Sci.* **1989**, *4*, 509–519. [[CrossRef](#)]
34. Muiambo, H.F.; Focke, W.W.; Atanasova, M.; Benhamida, A. Characterization of urea-modified Palabora vermiculite. *Appl. Clay Sci.* **2015**, *105–106*, 14–20. [[CrossRef](#)]
35. Suzuki, M.; Wada, N.; Hines, D.; Whittingham, M. Hydration states and phase transitions in vermiculite intercalation compounds. *Phys. Rev. B* **1987**, *36*, 2844. [[CrossRef](#)] [[PubMed](#)]